Generalized Graph Laplacian Based Anomaly Detection for Spatiotemporal μPMU Data

Mingjian Cui, *Senior Member, IEEE*, Jianhui Wang, *Senior Member, IEEE*, Anthony R. Florita, *Member, IEEE*, and Yingchen Zhang, *Senior Member, IEEE*

***Abstract*—This letter develops a novel anomaly detection method using the generalized graph Laplacian (GGL) matrix to visualize the spatiotemporal relationship of distribution-level phasor measurement unit (μPMU) data. The μPMU data in a specific time horizon is segregated into multiple segments. An optimization problem formulated as a Lagrangian function is utilized to estimate the GGL matrix. During the iterative process, an optimal update is constituted as a quadratic program (QP) problem. To perform the μPMU-based spatiotemporal analysis, normalized diagonal elements of GGL matrix are proposed as a quantitative metric. The effectiveness of the developed method is demonstrated through real-world μPMU measurements gathered from test feeders in Riverside, CA.**

***Index Terms*—Anomaly detection, distribution PMU (μPMU), graph Laplacian matrix, spatiotemporal analysis.**

I. Introduction

With the increasing development of distribution-level phasor measurement units (μPMUs), the real-time monitoring of distribution systems has been significantly improved with advanced sensor technologies. Three-phase voltage and current phasors with corresponding magnitude and angle information can be provided by GPS-synchronized measurements [1]. Synchronized voltage and current measurements at higher resolution and precision are capable of facilitating a high level of visibility for distribution systems [2]. Synchronized μPMU data-driven anomaly detection can contribute to numerous applications in distribution system operations. Farajollahi *et al*. [1] developed a method to locate the source of events in power distribution systems by using distribution-level μPMUs. Jamei *et al*. [3] detected the abnormal behavior in the control perimeter by focusing on μPMUs.

Unlike conventional μPMU event detection techniques, such as the CUSUM algorithm [3] which is highly dependent on a pre-defined threshold obtained by training a semi-supervised behavior-based detector, this letter attempts to capture affinity similarities and patterns among μPMU data by using a generalized graph Laplacian (GGL) matrix and the three-sigma rule. The μPMU data is represented by weighted graphs that can offer general and flexible representations for modeling affinity similarity among anomalies in μPMU data. Essentially, the similarity of μPMU data under normal conditions would be broken when anomaly events occur. Based on this concept, this letter seeks to address two critical questions for μPMU-based anomaly detection. (i) Is it possible to quantitatively represent the similarity between anomalies and the normal μPMU data with numerical metrics? (ii) Can users deploy the spatiotemporal similarity to identify system-wide anomalies? Toward this end, this letter develops a GGL based anomaly detection method for the spatiotemporal analysis and visualization. The main technical contributions of this letter are that: (i) using graph learning techniques to detect μPMU-based anomalies for the first time and (ii) analyzing spatiotemporal characteristics of anomalies using high-resolution μPMU data.

The organization of this letter is as follows. In Section II, the developed GGL method is briefly introduced with the pseudocode of generating GGL matrix. Case studies and result analysis performed on real-time μPMU data are discussed in Section III. Concluding remarks are summarized in Section IV.

M. Cui and J. Wang are with the Department of Electrical and Computer Engineering at Southern Methodist University, Dallas, TX, 75275 USA (email: {mingjiancui, jianhui}@smu.edu).

A. R. Florita and Y. Zhang are with the National Renewable Energy Laboratory (NREL), Golden, CO, 80401 USA (email: {anthony.florita, yingchen.zhang}@nrel.gov).

Manuscript received, 2018.

II. GGL Methodology

The increasing graph learning techniques pave a distinctive way for the anomaly detection using the streaming μPMU data with high resolution. Compared with the combinatorial graph Laplacians (CGLs), GGLs are shown to be more useful and practical [4]. GGL can maintain all the edges with positive weights and introduce additional connectivity due to negative weights [5]. To estimate the GGL matrix, the optimization problem using a Lagrangian function is constituted as:

$$\min\ L(\mathbf{\Theta}) = \|\mathbf{\Theta} \odot \mathbf{H}\|_1 + \|\mathbf{\Theta} \odot \mathbf{M}\|_1 - \operatorname{logdet}(\mathbf{\Theta}) \quad (1)$$

s.t.

$$\mathcal{L}(\mathbf{A}) = \left\{ \mathbf{\Theta} \in \mathcal{L} \;\middle|\; \begin{array}{l} (\mathbf{\Theta})_{ij} \le 0 \ \text{ if } \ (\mathbf{A})_{ij} = 1 \\ (\mathbf{\Theta})_{ij} = 0 \ \text{ if } \ (\mathbf{A})_{ij} = 0 \end{array} \right\}_{\forall i,j\ i \neq j} \quad (2)$$

where $\mathbf{H}$ is the regularization matrix and $\mathbf{H} = \alpha(\mathbf{I} - \mathbf{II})$. $\mathbf{I}$ is an identity matrix. $\mathbf{II}$ is an all-ones matrix. α is the regularization parameter. $\mathbf{\Theta}$ is the estimated GGL matrix. $\mathcal{L}$ is the target set of graph Laplacians. $\mathbf{A}$ is the similarity matrix. $\odot$ means the element-wise multiplication of two matrices. $\|\cdot\|_1$ means the sum of absolute values of all elements (ℓ_1-norm). $\operatorname{logdet}(\cdot)$ means the natural logarithm of a determinant. $\mathbf{M}$ is the Lagrange multiplier matrix. The similarity matrix $\mathbf{A}$ is calculated by the difference of $\mathsf{ddiag}(\mathbf{\Theta})$ and $\mathbf{\Theta}$:

$$\mathbf{A} = \mathsf{ddiag}(\mathbf{\Theta}) - \mathbf{\Theta} \quad (3)$$

The derivative of (1) with respect to $\mathbf{\Theta}$ is set to an all-zeros matrix $\mathbf{O}$, given by:

$$\mathrm{d}L(\mathbf{\Theta})/\mathrm{d}\mathbf{\Theta} = -\mathbf{\Theta}^{-1} + \mathbf{K} + \mathbf{M} = \mathbf{O} \quad (4)$$

where $\mathbf{K} = \mathbf{S} + \mathbf{H}$ and $\mathbf{S}$ is the covariance matrix empirically obtained from μPMU data samples.

Letting the inverse matrix $\mathbf{C} = \mathbf{\Theta}^{-1}$ and using the formula in (4), the optimality condition for the uth row/column of $\mathbf{\Theta}$, given by:

$$-\mathbf{c}_u + \mathbf{k}_u + \mathbf{m}_u = \mathbf{o} \quad (5)$$

$$-c_u + k_u + m_u = 0 \quad (6)$$

where $\mathbf{c}_u$, $\mathbf{k}_u$, and $\mathbf{m}_u$ are vectors obtained from the uth row (or column) of matrices $\mathbf{C}$, $\mathbf{K}$, and $\mathbf{M}$, respectively. c_u, k_u, and m_u are scalars obtained from the uth diagonal of matrices $\mathbf{C}$, $\mathbf{K}$, and $\mathbf{M}$, i.e., $c_u = (\mathbf{C})_{uu}$, $k_u = (\mathbf{K})_{uu}$, and $m_u = (\mathbf{M})_{uu}$, respectively.

Based on the above optimality conditions, an optimal update is designed for the uth row/column of $\boldsymbol{\Theta}$ as a quadratic program (QP) problem, given by:

$$\min_{\boldsymbol{\beta}} \ \boldsymbol{\beta}^{\mathrm{T}}\mathbf{Q}\boldsymbol{\beta}/2 - \boldsymbol{\beta}^{\mathrm{T}}\mathbf{p} \tag{7}$$

where $\boldsymbol{\beta} = -(\boldsymbol{\theta}_u)_{\mathcal{S}}$, $\mathbf{p} = (\mathbf{k}_u/k_u)_{\mathcal{S}}$, and $\mathbf{Q} = \left(\boldsymbol{\Theta}_u^{-1}\right)_{\mathcal{S}\mathcal{S}}$. Vectors/matrix $\boldsymbol{\beta}$, $\mathbf{p}$, and $\mathbf{Q}$ are selected from the original variable vectors/matrix $\boldsymbol{\theta}_u$, $\mathbf{k}_u/k_u$, and $\boldsymbol{\Theta}_u^{-1}$ based on the index set $\mathcal{S}$.

The pseudocode in Algorithm 1 is shown to solve the desired GGL matrix. It iteratively updates each row/column of the estimated GGL matrix $\widehat{\boldsymbol{\Theta}}$ and its estimated inverse matrix $\widehat{\mathbf{C}}$ by optimizing the QP problem formulated in (7). The convergence criterion is defined as the sum of squared values of GGL matrix elements in the vth iteration:

$$\frac{\|\widehat{\boldsymbol{\Theta}}_v - \widehat{\boldsymbol{\Theta}}_{v-1}\|_F}{\|\widehat{\boldsymbol{\Theta}}_{v-1}\|_F} = \sqrt{\sum_{i=1}^{N}\sum_{j=1}^{N}\left|\widehat{\theta}_{ij,v}\right|^2} - \sqrt{\sum_{i=1}^{N}\sum_{j=1}^{N}\left|\widehat{\theta}_{ij,v-1}\right|^2} \tag{8}$$

III. Case Studies and Results

A. μPMU Data Description and Preprocessing

The performance of our developed method is validated using μPMU data from four real-world distribution feeder and building locations in Riverside, CA [1]. Distribution μPMU devices are used to collect the synchrophasor data of the voltage and current data with a 60 Hz sampling rate. In this letter, it is assumed that each data segment spans approximately 20 seconds and the total number of segments is 37, which corresponds to an approximately 97% true positive rate (*TPR*) of detecting anomalies. The μPMU data is preprocessed to filter the ambient noise using ℓ_1 *trend filtering*, which is a simple and tractable technique for generating piecewise linear fits to the original data by solving a convex program [7].

Algorithm 1: Iterative Process for Getting GGL Matrix

Preprocess μPMU data to filter the ambient noise. Obtain sample statistics $\mathbf{S}$. Set the regularization matrix $\mathbf{H}$ and $\mathbf{K} = \mathbf{S} + \mathbf{H}$ with a tolerance ϵ. The total number of μPMU segments is set as N.
Initialize estimated inverse matrix $\widehat{\mathbf{C}}$ as the diagonal matrix formed by diagonal elements of $\mathbf{K}$; and estimated GGL matrix is set as $\widehat{\boldsymbol{\Theta}} = \widehat{\mathbf{C}}^{-1}$.
for *Iteration* v *from* 1 *to* N_v **do**
  Assign the previous estimated $\widehat{\boldsymbol{\Theta}}_{v-1} \leftarrow \widehat{\boldsymbol{\Theta}}$
  for *Iteration* u *from* 1 *to* N **do**
    Partition $\widehat{\boldsymbol{\Theta}}$, $\widehat{\mathbf{C}}$, and $\mathbf{K}$ for u using the matrix inversion lemma [6].
    Update $\widehat{\boldsymbol{\Theta}}_u^{-1} = \widehat{\mathbf{C}}_u - \widehat{\mathbf{c}}_u\widehat{\mathbf{c}}_u^{\mathrm{T}}/\widehat{c}_u$; estimate $\widehat{\boldsymbol{\beta}}$ using (7) to update the uth vector $\widehat{\boldsymbol{\theta}}_u$ and scalar $\widehat{\theta}_u$; and update $\widehat{\mathbf{C}}_u$, $\widehat{\mathbf{c}}_u$, and $\widehat{c}_u$ using:
$$\widehat{\mathbf{C}}_u = \widehat{\boldsymbol{\Theta}}_u^{-1} + \widehat{\mathbf{c}}_u\widehat{\mathbf{c}}_u^{\mathrm{T}}/\widehat{c}_u;\ \widehat{\mathbf{c}}_u = -\widehat{\mathbf{C}}_u\widehat{\boldsymbol{\theta}}_u/\widehat{\theta}_u$$
$$\widehat{c}_u = 1/(\widehat{\theta}_u - \widehat{\boldsymbol{\theta}}_u^{\mathrm{T}}\widehat{\boldsymbol{\Theta}}_u^{-1}\widehat{\boldsymbol{\theta}}_u)$$
    Rearrange estimated $\widehat{\boldsymbol{\Theta}}$ and its inverse $\widehat{\mathbf{C}}$.
  end
  Calculate the convergence criterion and update: $\widehat{\boldsymbol{\Theta}}_v \leftarrow \widehat{\boldsymbol{\Theta}}$; $v \leftarrow v+1$
  if *convergence criterion in* (8) *is less than* ϵ **then**
    break
  end
end

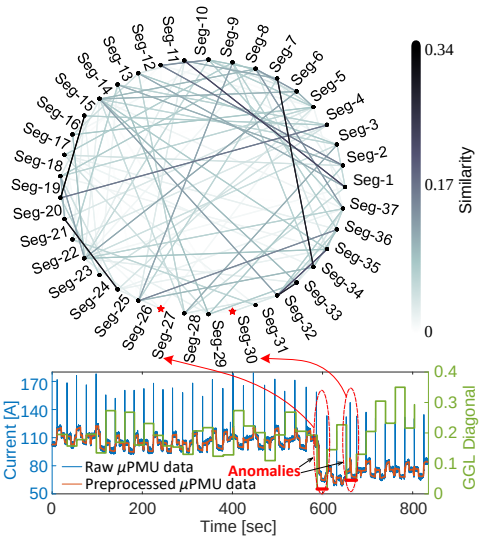

Fig. 1. Visualization of current data anomalies of Phase a at Location 1.

B. Detected Anomalies in Temporal Domain

Fig. 1 shows the visualization of current data of Phase a at Location 1 with two anomaly events. As shown in the bottom subfigure, the preprocessed current data without ambient noise (orange line) is used to detect the anomalies. The first anomaly (27$^{\text{th}}$ segment) is shown as a smooth-curve event [8] and challenging to detect for operators. It is mainly because this smooth-curve anomaly presents a smooth and continuous coupling together with adjacent points of current data. The second anomaly (30$^{\text{th}}$ segment) is shown as a small pulse event [8]. The green line indicates the diagonal elements of estimated GGL matrix $\widehat{\boldsymbol{\Theta}}$. As shown in the top subfigure, a deeper color means a higher similarity between two segments. Both segments 27 and 30 almost do not have similarity with any other segments (see lines connected with Seg-27 and Seg-30 denoted by the lack of colors) due to the occurrence of anomalies. By comparing subfigures in Fig. 1, the accuracy of detected anomalies using GGL can be validated.

Table I sorts the metric of the GGL matrix's diagonal elements, $\mathrm{diag}(\widehat{\boldsymbol{\Theta}})$, with the first four segments. The threshold of this metric is determined by the empirical three-sigma rule [9]. Based on experimental experience in this case, we use the 1.2-sigma rule to obtain thresholds. If the metric is less than the threshold, anomalies are detected. As can be seen, segments 27 and 30 with anomalies show the smallest values (see the

TABLE I
Metrics of First Four Segments of Phase a at Location 1

	Sort of Metrics				Threshold
$\mathrm{diag}(\widehat{\boldsymbol{\Theta}})$	0.0176	0.0680	0.1549	0.1698	0.1537
Segments	Seg-27	Seg-30	Seg-22	Seg-5	

TABLE II
TPR AND *FPR* RESULTS USING CUSUM AND GGL

Methods	*TPR* [%]	*FPR* [%]
CUSUM	93.33	3.33
$\mathsf{diag}(\widehat{\boldsymbol{\Theta}})$ (***proposed***)	96.67	1.67

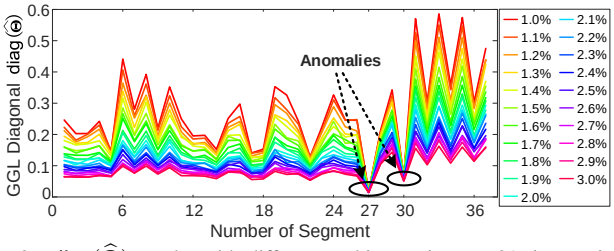

Fig. 2. $\mathsf{diag}(\widehat{\boldsymbol{\Theta}})$ results with different ambient noises on 21 time series of μPMU data.

red area). This observation verifies that the developed method based on GGL matrix is accurate for anomaly detection in μPMU data.

To compare our method with the CUSUM method in [3], the *TPR* and false positive rate (*FPR*) are used for illustration. Table II shows the quantitative results of *TPR* and *FPR*. Larger *TPR* and smaller *FPR* mean a better performance of the detection method. As shown in this table, the $\mathsf{diag}(\widehat{\boldsymbol{\Theta}})$ metric validates the effectiveness of the proposed method.

To show the robustness of the developed approach, 21 time series of μPMU data are collected and added by a Gaussian random noise with a zero mean and a standard deviation of a proportion λ of the corresponding μPMU data. λ is increased from 1% to 3% with a step of 0.1% (i.e., $\lambda \in [1\%, 3\%]$). Fig. 2 shows the results of $\mathsf{diag}(\widehat{\boldsymbol{\Theta}})$ with different ambient noises. As seen from top to bottom in the vertical axis, the similarity (GGL diagonal) among μPMU segments is gradually reduced with ambient noises denoted by the increasing proportion λ. However, anomalies on segments 27 and 30 are entirely detected for all 21 time series. This observation can validate the robustness of the developed approach with respect to ambient noises.

C. Spatiotemporal Analysis of Detected Anomalies

The three-phase current and voltage data at four locations are used for the spatiotemporal analysis of detected anomalies. Other information of μPMU data is introduced in Section III-A. The normalized diagonal element of GGL matrix, $\mathsf{diag}(\widehat{\boldsymbol{\Theta}})$, is proposed as a metric for quantifying spatiotemporal relationship, given by:

$$\overline{\mathsf{diag}(\widehat{\boldsymbol{\Theta}})} = \frac{\mathsf{diag}(\widehat{\boldsymbol{\Theta}}) - \min(\mathsf{diag}(\widehat{\boldsymbol{\Theta}}))}{\max(\mathsf{diag}(\widehat{\boldsymbol{\Theta}})) - \min(\mathsf{diag}(\widehat{\boldsymbol{\Theta}}))} \tag{9}$$

Fig. 3 visualizes the spatiotemporal relationship of μPMU data by using the metric $\mathsf{diag}(\widehat{\boldsymbol{\Theta}})$. As seen in this figure, each phase has the same metric value (color) among three phases under most circumstances. However, for Phase b current at Location 2 in Seg-34, it is possible that one single-phase current event occurs. We can also see several three-phase current events that occur at Location 3 and 4. For Location 1 and 2, there are two current/voltage events in Seg-21 and Seg-27, respectively. In Seg-7, there is a system-wide voltage-stability event that occurs at all four locations with a deeper color. Theoretically, voltage-stability anomalies routinely occur due

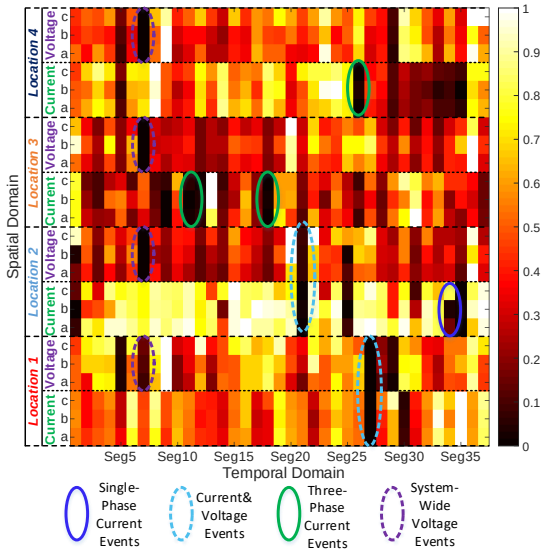

Fig. 3. Spatiotemporal visualization of anomalies using the normalized diagonal elements of GGL matrix $\widehat{\boldsymbol{\Theta}}$.

to reactive power events caused by distribution generators, capacitors, or reactors. Current events are primarily caused by distribution generator trips, line faults, etc.

IV. CONCLUSION

In this letter, we develop a novel μPMU-based anomaly detection method by using a generalized graph Laplacian (GGL) matrix. The developed detection method utilizes a Laplacian optimization function to estimate the GGL matrix. A quadratic program technique is used to design the optimal update during the computation process. In addition, the normalized diagonal elements of GGL matrix are proposed as a metric for the spatiotemporal analysis of μPMU data. Some observations are shown as follows:

(i) The developed method is able to accurately and robustly detect the anomalies in the temporal domain.
(ii) The spatiotemporal affinity of system-wide anomalies can be clearly characterized and visualized for operators.

ACKNOWLEDGMENT

This work was authored in part by Alliance for Sustainable Energy, LLC, the Manager and Operator of the National Renewable Energy Laboratory for the U.S. Department of Energy (DOE) under Contract No. DE-AC36-08GO28308. Funding provided by the U.S. Department of Energy Grid Modernization Lab Consortium. The views expressed in the article do not necessarily represent the views of the DOE or the U.S. Government. The U.S. Government retains and the publisher, by accepting the article for publication, acknowledges that the U.S. Government retains a nonexclusive, paid-up, irrevocable, worldwide license to publish or reproduce the published form of this work, or allow others to do so, for U.S. Government purposes.

REFERENCES

[1] M. Farajollahi, A. Shahsavari, E. Stewart, and H. Mohsenian-Rad, "Locating the source of events in power distribution systems using micro-PMU data," *IEEE Trans. Power Syst.*, vol. 33, no. 6, pp. 6343–6354, 2018.
[2] H. Mohsenian-Rad, E. Stewart, and E. Cortez, "Distribution synchrophasors: pairing big data with analytics to create actionable information," *IEEE Power Energy Mag.*, vol. 16, no. 3, pp. 26–34, 2018.

[3] M. Jamei, A. Scaglione, C. Roberts, E. Stewart, S. Peisert, C. McParland, and A. McEachern, "Anomaly detection using optimally placed μPMU sensors in distribution grids," *IEEE Trans. Power Syst.*, vol. 33, no. 4, pp. 3611–3623, 2018.
[4] T. Biyikoglu, J. Leydold, and P. F. Stadler, *Laplacian eigenvectors of graphs: Perron-Frobenius and Faber-Krahn type theorems*. Springer, 2007.
[5] H. E. Egilmez, E. Pavez, and A. Ortega, "Graph learning from data under Laplacian and structural constraints," *IEEE J. Sel. Top. Signal Process.*, vol. 11, no. 6, pp. 825–841, 2017.
[6] M. A. Woodbury, "Inverting modified matrices," *Memorandum report*, vol. 42, no. 106, p. 336, 1950.
[7] S. J. Kim, S. Boyd, and D. Gorinevsky, "ℓ_1 trend filtering," *SIAM Rev.*, vol. 51, no. 2, pp. 339–360, 2009.
[8] M. Cui, J. Wang, and M. Yue, "Machine learning based anomaly detection for load forecasting under cyberattacks," *IEEE Trans. Smart Grid*, 2019, in press.
[9] F. Pukelsheim, "The three sigma rule," *The American Statistician*, vol. 48, no. 2, pp. 88–91, 1994.